

# RSC Advances



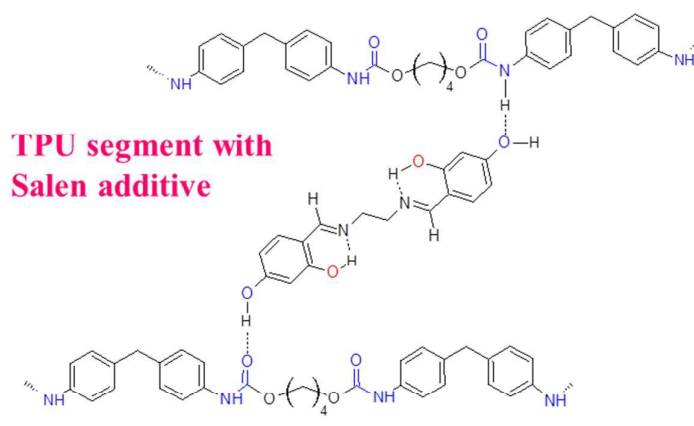
This is an *Accepted Manuscript*, which has been through the Royal Society of Chemistry peer review process and has been accepted for publication.

*Accepted Manuscripts* are published online shortly after acceptance, before technical editing, formatting and proof reading. Using this free service, authors can make their results available to the community, in citable form, before we publish the edited article. This *Accepted Manuscript* will be replaced by the edited, formatted and paginated article as soon as this is available.

You can find more information about *Accepted Manuscripts* in the [Information for Authors](#).

Please note that technical editing may introduce minor changes to the text and/or graphics, which may alter content. The journal's standard [Terms & Conditions](#) and the [Ethical guidelines](#) still apply. In no event shall the Royal Society of Chemistry be held responsible for any errors or omissions in this *Accepted Manuscript* or any consequences arising from the use of any information it contains.

## Graphical abstract



### Under fire Scenario

**TPU**



**TPU+additive**



**Fire protection by intumescence**

**Resorcinol based Salen framework as non-phosphorus and non-halogen fire retardant additive for thermoplastic polyurethane (TPU).**

## Salen based Schiff bases to flame retard thermoplastic polyurethane mimicking operational strategies of thermosetting resin

Cite this: DOI: 10.1039/x0xx00000x

Received 00th January 2012,  
Accepted 00th January 2012

DOI: 10.1039/x0xx00000x

www.rsc.org/

Anil D. Naik, Gaëlle Fontaine, Séverine Bellayer, and Serge Bourbigot\*

A classical Schiff base *N,N'*-bis(4-hydroxysalicylidene)ethylenediamine (L2), member of Salen group that has been introduced as a non-phosphorus and non-halogen flame retardant in thermoplastic polyurethane (TPU) is found to operate in an intriguing way to fire retard the material. L2 blended with TPU significantly improves the inherent flammability of TPU without synergist. The plausible mechanism including intermediates in the reinforcement of this elastomer towards flame retardancy is elaborated in line with char forming abilities of this  $\beta$ -resorcyaldehyde based Schiff base. Conclusions were drawn based on the input from thermal, spectroscopic, microscopic and operando spectroscopic techniques. While its unsubstituted counterpart, *N,N'*-bis(salicylidene)ethylenediamine (L1) lags behind in performance, its structural isomer *N,N'*-bis(5-hydroxysalicylidene)ethylenediamine (L3) is equally efficient but exhibits another mechanism of action. The performance of L2-TPU is found to be mainly in condensed phase and is due to decoding of intrinsic cross linking ability of the key building block of the additive i.e. resorcinol via structural transformation over a range of temperature. This results in methylene bridged phenolic resin type material having high temperature stability. The process is also found to interfere with TPU unzipping process delaying its thermal degradation and favor extensive cross-linking promoting char formation with insulative properties.

### 1. Introduction

Thermoplastic polyurethane (TPU) belongs to thermoplastic elastomers that combine the mechanical properties of vulcanized rubber with the processability of thermoplastic polymers and are considered to be the most versatile polymers.<sup>1-2</sup> They are used in a wide variety of applications including adhesives, sealants, coatings, fibers, injection molded components, thermoplastic parts, industrial cables, energy exploration, automotive, transportation etc.<sup>1-5</sup> On the downside the flammability of PU materials presents a threat to both the performance and integrity of the product. Further fire degraded products contribute to environmental pollution and health risks. Considering these facts coupled with regulatory issues, flame retardancy in PU has become a necessity as well as an obligation.<sup>6-9</sup> To tackle these issues, flame retardants (FRs) are added to the PU system which may or may not be part of the PU macromolecular system. Depending upon the type of FR, they would exert varying influences on quenching, delaying, minimizing or retarding the burning process. Wide array of additives ranging from inorganic fillers to composites has been employed in this direction.<sup>1-6, 10-23</sup> Inorganic oxides, hydroxides and carbonates; organic and inorganic derivatives of boron,

silicon, phosphorus and melamine; and expandable graphite to name some. On economic and efficiency scale, intumescence promoting FRs is proposed to be highly desirable. An intumescence is a protection mechanism of the FR involving the formation of an expanded foamy char. Thus formed carbonaceous char acts as physical barrier to heat, air and pyrolysis products protecting the underlying polymer.<sup>6-9</sup> This constitutes condensed phase of action in flame retardancy. FRs are also capable of acting in gas phase by various mechanism.<sup>6-9</sup> Recently Fontaine et al<sup>4</sup> introduced a non-halogen, non-phosphorus, and relatively simple organic framework of 'Salen' (Figure 1a) and their metal chelates to the flame retardancy of thermoplastic polyurethane elastomer (Figure 1b) triggering the entry of Schiff bases for high temperature applications. The nominal dosage of 10wt.-% and absence of any synergist are creditable features which results in significant reduction in peak of heat release rate.

In order to expand the applicability of this FR system it is necessary to understand the underlying physical and chemical aspects leading to flame retardancy, particularly by metal free 'Salen' systems. It is the main goal of this paper.

## ARTICLE

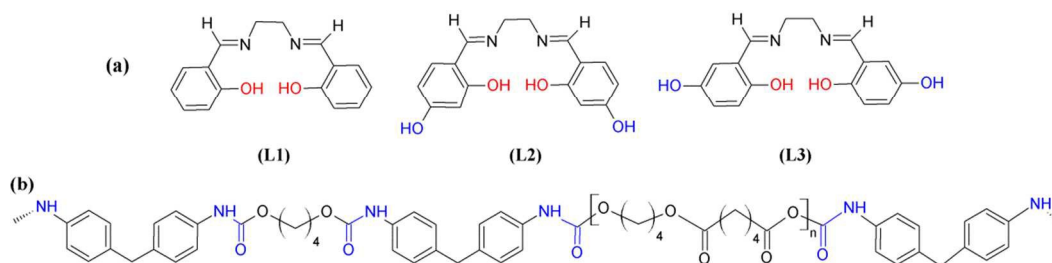


**Figure 1.** (a) *Salen* based Schiff base additives (b) Framework of thermoplastic polyurethane.

We have prepared three Schiff bases (L1-L3). L1 represents the simplest framework among them and assumed to have limited H-bonding network. L2 and L3 have hydroxy group at 4 and 5 position respectively on the aromatic group due to which they can expand the supramolecular interaction by intermolecular H-bonding. L1-L3 were blended in TPU and the resulting formulations were characterized by FTIR,  $^{13}\text{C}$  MAS NMR, TGA, DSC and microscopic techniques. Pyrolysis flow combustion calorimetry (PCFC), cone calorimetry and limiting oxygen index (LOI) are the evaluating tools for fire properties. The observed flame retardancy is broadly discussed examining condensed phase and gas phase mode of action to elucidate the mechanism of flame retardancy. Samples for the condensed phase analysis were collected from cone calorimetry experiment which represents different stages of degradation and studied by FTIR,  $^{13}\text{C}$  MAS NMR, SEM and EPMA. Gas phase analysis were studied by TGA coupled FTIR and py-GCMS. A comprehensive study is given in the following section on how a structured Schiff base could reinforce TPU thermally, chemically and physically in contending fire risks.

## 2. Experimental

### 2.1. Materials

Thermoplastic Polyurethane (Elastollan C85A) was kindly supplied by BASF. N,N'-bis(salicylidene)ethylenediamine (L1) and N,N'-bis(4-hydroxysalicylidene)ethylenediamine (L2) and N,N'-bis(5-hydroxysalicylidene)ethylenediamine (L3) were synthesized based on earlier report.<sup>4</sup>

### 2.2. Formulations, processing and sampling

#### 2.2.1. Formulation and processing:

TPU is dried for at least 12 hours at 80°C before use. Compounding of formulations with 10 % of additives were performed using HAAKE Rheomix OS PTW 16 blender.<sup>4</sup> The

temperature of the mixer was set at 180°C and the shear was 50 rpm for 10 minutes. These blended mixture were ground in liquid nitrogen in an ultracentrifuge mill to produce a powder and dried at 80 °C under vacuum for 12 h before use. TPU used for comparison in this study is also processed under same condition.

#### 2.2.2. Sampling:

Samples for the degradation studies were collected from cone calorimetry experiment which is based on HRR curve wherein sample (100 x 100 x 3 mm<sup>3</sup> plates) exposure to heat flux were stopped and withdrawn at the onset, peak, descending, and end of HRR curve. A 4x4cm piece is scooped out from the central part of these plates including the intumescence part. Residue are manually crushed and collected. Other samples are semi-solid and are cut into small pieces and ground in liquid nitrogen in an ultracentrifuge mill to produce a powder. Samples were dried at 100 °C under vacuum for 12 h and stored. These samples are used for all the analysis.

### 2.3. Instrumental

#### 2.3.1. Thermal analysis:

Thermogravimetric analyses (TGA) were performed using SDT Q600 (TA instruments). Samples (approx. 6-7 mg) were placed in open alumina pans and heated under nitrogen atmosphere (100mL/min) with a heating rate of 10°C/min.

#### 2.3.2. Mass loss cone calorimeter:

The mass loss cone calorimeter (Fire Testing Technology (FTT)) is used for recording HRR curve and collecting sample for analysis for condensed phase. Plates (100x100x3mm<sup>3</sup> plates) for cone calorimeter test were made via compression molding using DARRAGON press apparatus. Plates were wrapped in aluminium foil leaving the upper surface exposed to the heater and placed in horizontal position on ceramic block encased in a metallic container at a distance of 35mm from

cone base. External heat flux of  $35\text{ kW/m}^2$  was used for all the experiments.

### 2.3.3. Spectral and microscopy analysis:

FT-IR were recorded on Nicolet Impact 400 D in ATR mode at room temperature.  $^{13}\text{C}$  NMR measurements have been performed on a Bruker Avance II 400 at 100.4 MHz using 3.2mm probes, with cross polarization (CP)  $^1\text{H}$ - $^{13}\text{C}$ , dipolar decoupling (DD) and magic angle spinning (MAS) at a spinning speed of 14kHz. For all samples, a delay time between two impulsions of 5 s and a contact time of 1ms were used. VHX digital optical microscope (Keyence, VH-Z 100R) was used to investigate texture of samples. The surface of the sample for EPMA was prepared with a Leica Ultracut ultramicrotome at cryo temperature with a diatome diamond knife. The image were taken with a Cameca SX100 EPMA in BSE mode at 15kV 15 nA. Morphology of char was studied using scanning electron microscope (SEM) (Field emission gun (FEG) Hitachi S4700) at 6 kV at different magnifications. The surface of the residue was taped on an aluminium SEM plate and carbon coated with a Baltec SCD005 sputter coater

### 2.3.4. TGA-FTIR analysis:

Gas phase analysis were carried out in TGA Q5000 (TA instruments) coupled with FTIR Nicolet spectrometer (ThermoFischer). Samples (~10mg) were heated in a 100  $\mu\text{L}$  alumina crucible from  $50^\circ\text{C}$  to  $800^\circ\text{C}$  with a heating rate of  $10^\circ\text{C}/\text{min}$  under nitrogen atmosphere. A balance purge flow of 15 mL/min and a sample purge flow of 100mL/min was maintained. A transfer line with an inner diameter of 1mm was used to connect TGA and infrared cell. The temperature of transfer line and gas cell was kept at  $225^\circ\text{C}$ . Prior to this, samples were kept for 2h under nitrogen stream. IR spectra were collected in  $400\text{--}4000\text{ cm}^{-1}$  spectral range.

### 2.3.5. Pyrolysis GCMS:

Samples (~200  $\mu\text{g}$ ) were analyzed by Pyrolysis GC-MS (Shimadzu, GCMS-QP2010 SE). GC separation was carried out with a fused silica capillary column (SLB 5ms) of 30m length and  $0.25\mu\text{m}$  thickness. Analyses were carried out both in direct pyrolysis mode and desorption method. The temperature selection for desorption is based TGA pattern of concerned sample with a heating rate of  $10^\circ\text{C}/\text{min}$ . The initial column temperature was held at  $35^\circ\text{C}$  for a period that corresponds to desorption time followed by a temperature ramp at  $10^\circ\text{C}/\text{min}$  to a final temperature of  $300^\circ\text{C}$  and isotherm for 20 min. For direct pyrolysis the furnace is set for the final temperature ( $600^\circ\text{C}$  which corresponds to completion of second major degradation step) and sample is pyrolysed for 0.5 min. Column oven temperature is programmed in the following way. The initial column temperature was held at  $35^\circ\text{C}$  for 1 min. followed by a temperature ramp at  $10^\circ\text{C}/\text{min}$  to a final temperature of  $300^\circ\text{C}$  and isotherm for 20 min. Helium was

used as a carrier gas at pressure of 120kPa with a split ratio of 50. The transfer line was maintained at  $275^\circ\text{C}$ . The MS was operated under Electron Ionization EI mode. An online computer using GCMS real time analysis and PY-2020i software controlled GC/MS system. The eluted components were identified by library search and only significant peaks observed in the total ion chromatograms were studied and compared to a mass spectral database (GCMS postrun analysis, and NIST).

## 3. Results and discussion

### 3.1. Thermoplastic polyurethane, additives and formulations

Thermoplastic polyurethane elastomers (TPUs) are manufactured by reacting a diisocyanate, a macroglycol and a chain extender. The framework of TPU (Figure 1b) consists of block copolymers of, soft segment (SS) and hard segments (HS) with a repeating unit of urethane linkage ( $-\text{NHC}(=\text{O})\text{O}-$ ). The HS are produced by the reaction between the diisocyanate (eg. 4,4'-methylene diphenyl diisocyanate (MDI)) and the chain extender (eg. butanediol), and are responsible for rigidity, and are highly polar and present a relatively high melting temperature. HSs have high interchain interactions due to hydrogen bonding between the urethane groups. On the other hand, the SS consist of long polyester chains interconnecting two HS. This relatively non-polar segment impart flexibility and elastomeric properties to the TPU and present a relatively low softening temperature. The differences in polarity between hard and soft segments produce phase separation in the TPUs structure, giving micro-domains. TPUs will be elastic in the range of temperature between the glass transition temperature ( $T_g$ ) generally located at about  $-60^\circ\text{C}$  and the softening temperature of the elastomeric domains ( $60\text{--}100^\circ\text{C}$ ). Source of TPU in our study is Elastollan (C85A) which is a thermoplastic polyurethane elastomer containing polyester chains.<sup>5</sup> Flame retardants (L1-L3) used in our study are classical Schiff bases and quite a large number of publications are available in the literature on their synthesis and properties.<sup>4</sup> Their syntheses were performed in ethanol and are isolated as crystalline materials. Their thermal degradation and associated changes in physical and chemical properties are studied by us.<sup>24</sup> L1 is found to have least thermal stability among all, melting at  $128^\circ\text{C}$  followed by decomposition. Both L2 and L3 have better thermal stability, exhibit thermochromism and intriguing structural transformation associated with weight loss. Blending of L1-L3 in TPU was performed with a dosage of 10wt.-% as reported before.<sup>4</sup> Bright yellow color of L1 impart yellow color in L1-TPU, yellow-orange color of L2 to red color in L2-TPU and beige color of L3 to yellowish-brown to L3-TPU. We have particularly focused on resorcinol based 'Salen' additive (L2, Figure 1a) in TPU as resorcinol is known for its extraordinary ability of cross-linking and radical chemistry.<sup>22,23</sup> Thus present study is focused on L2-TPU with occasional reference to L1-TPU and L3-TPU.

### 3.2. Spectroscopic characterization

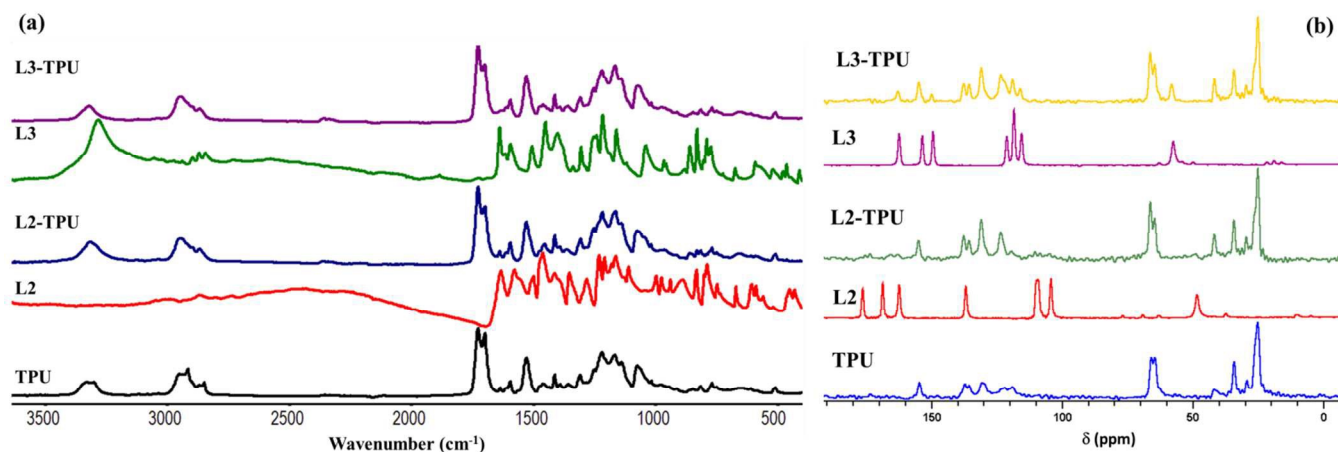


**Figure 2.** (a) FTIR spectra (b)  $^{13}\text{C}$  MAS NMR on TPU, selected additives and formulations.

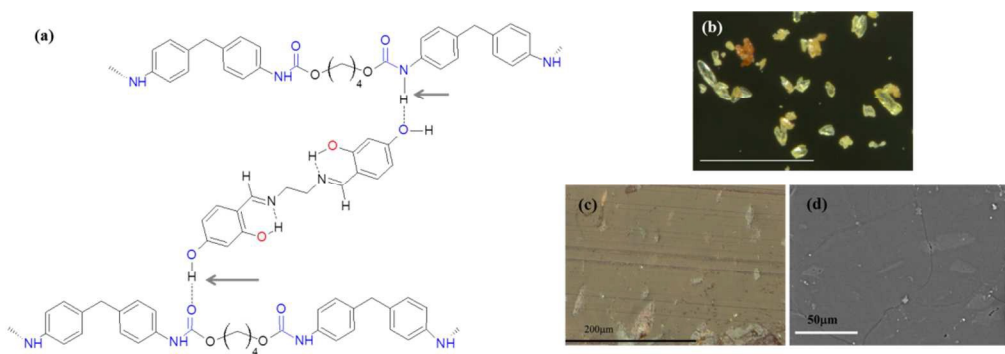


**Figure 3.** (a) Possible interchain H-bonding (focused by arrows) by Schiff base L2 (or L3) between urethane group of TPU. Part of the PU macromolecular chain is shown. (b) crystalline sample of L2 as observed under optical microscope. (c) Optical microscope image showing distribution of L2 in TPU (d) BSE image showing L2 additive as light colored aggregates in TPU matrix.

Selected FTIR of TPU and formulations are compared in figure 2a. Spectral pattern are similar except following changes. The -NH doublet ( $3331, 3305\text{ cm}^{-1}$ ) in TPU is replaced by a broad peak at  $3320\text{ cm}^{-1}$  in formulations due to disruption in H-bonding network caused by renewed H-bonding by additives. In the -CH absorption region sharp signals at  $2922$  and  $2852\text{ cm}^{-1}$  bands disappear while their shoulder bands ( $2950, 2870\text{ cm}^{-1}$ ) are retained. The band at  $1704\text{ cm}^{-1}$  (due to  $-\text{C}=\text{O}$  stretching vibration of urethane), decreases in intensity but the  $-\text{C}=\text{O}$  stretch of polyol signal ( $1727\text{ cm}^{-1}$ ) is unaffected.<sup>10-12,16</sup>  $^{13}\text{C}$  MAS NMR of TPU shows (Figure 2b) following signals: -carbonyl carbon at  $154.4\text{ ppm}$ ; aromatic carbons between  $137-118\text{ ppm}$ ; a doublet at  $65\text{ ppm}$  and multiplet between  $24.9-41.6\text{ ppm}$  belonging to  $-\text{CH}_2$  carbons. L3 bands (azomethine at

$162.7\text{ ppm}$ , aromatic carbons between  $110-155\text{ ppm}$ ,  $-\text{CH}_2$  carbon at  $57\text{ ppm}$ ) are detected in L3-TPU but with slight change in intensity and position although L2 bands (azomethine at  $176.1\text{ ppm}$ , aromatic carbons at  $168.5-104\text{ ppm}$ ;  $-\text{CH}_2$  at  $48.2\text{ ppm}$ ) are less resolved in L2-TPU. Based on the observed FTIR spectral change in the region of  $-\text{NH}$  and carbonyl group of urethane group it is assumed that, 'Salen' additives establish intra and interchain H-bonding interaction between urethane groups which bear both H-bonding acceptor and donor group. A tentative supramolecular interaction is shown in Figure 3a focusing on HS region. Long polyester chain of soft segment with only H-acceptor groups is expected to form limited H-bonding with Salen molecules.

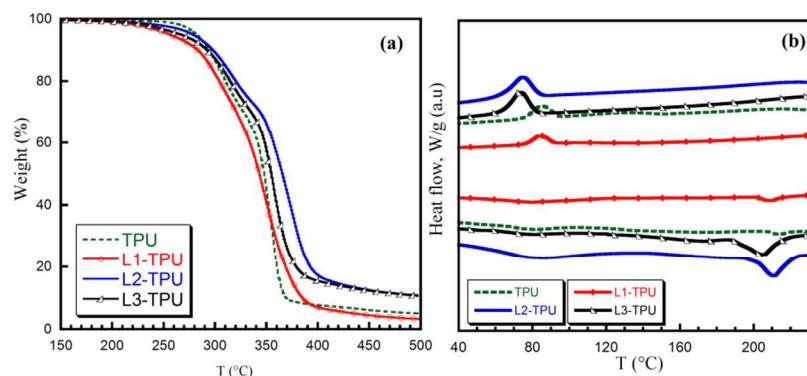


**Figure 4.** (a) Thermal decomposition in TPU and formulations (b) DSC profile of TPU and formulations.

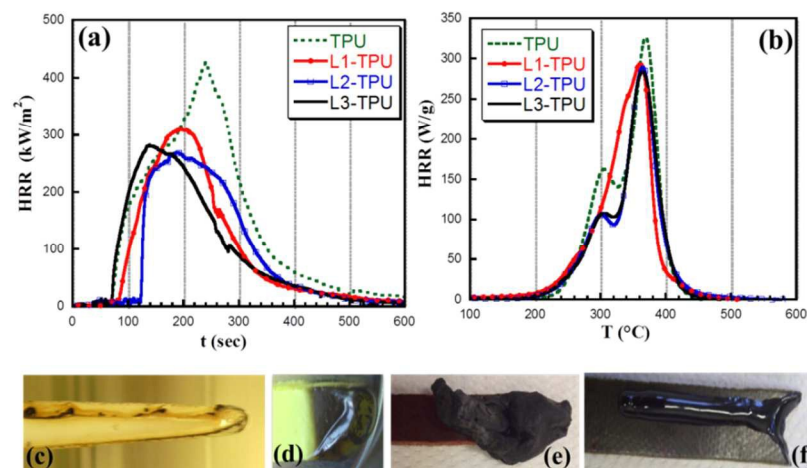


**Figure 5.** (a) HRR curve obtained from Cone calorimetry. (b) HRR curve obtained from PCFC (c-f) Physical response to flaming under LOI condition (c) neat TPU (d) L1-TPU (e) intumescence in L2-TPU (f) dripping in L3-TPU.

### 3.3. Thermal properties of formulations

Thermal decomposition behavior of TPU, and formulations are shown in figure 4a. The initial thermal stability (until  $\sim 260^{\circ}\text{C}$ ) of TPU and additives filled TPU are in the order  $\text{TPU} > \text{L2-TPU} > \text{L3-TPU} > \text{L1-TPU}$  (Table 1). TPU is found to be stable until  $250^{\circ}\text{C}$  and begin to lose weight gradually decomposing in two overlapping steps. The first major decomposition step is between  $275\text{--}340^{\circ}\text{C}$  although there is sluggish weight loss prior to this. The second major step of decomposition is more abrupt than the first step and takes place until  $374^{\circ}\text{C}$ . On the other hand, formulations (L2-TPU and L3-TPU) begin to lose weight early (around  $\sim 220^{\circ}\text{C}$ ) but subsequent decomposition steps are gradual extending the complete decomposition above  $400^{\circ}\text{C}$ . Residue weights are in the order  $\text{TPU-L1} < \text{TPU} < \text{TPU-L2} = \text{TPU-L3}$

suggesting char formation in L2-TPU and L3-TPU. It is intriguing that char formation takes place despite absence of an acid source. Although it has been found from our studies<sup>24</sup> that L2 and L3 themselves are capable of forming char, in the present case an interaction between Salen and TPU matrix can be envisioned. Although the initial thermal stability of formulations (de-stabilizing effect) is less, subsequent decomposition steps are shifted to higher temperature. The hardly indistinguishable two steps in TPU are also segregated in these formulations. The first weight loss during thermal degradation of TPU is due to the degradation of hard segment as a consequence of the relatively low thermal stability of urethane groups whereas the second weight loss has been associated to soft segment decomposition.<sup>2</sup>

## ARTICLE

**Table 1.** Thermal properties (TGA and DSC) of TPU and formulations.

Materials	TGA				DSC	
	Weight loss (%) at 262°C	Onset of 2 <sup>nd</sup> step	End of 2 <sup>nd</sup> step (°C)	Residue <sup>1</sup> (%) (at 450°C)	Heating (°C)	Cooling (°C)
TPU	1.5	330	374	6.0±0.12	177, 213	81
L1-TPU	6.0	336	396	4.4±0.13	79, 180, 209	84
L2-TPU	3.1	344	406	12.2±0.11	83, 170, 208	72
L3-TPU	4.6	342	391	12.1±0.12	76, 170, 203	74

<sup>1</sup>standard deviation given.**Table 2.** Fire properties derived from mass loss calorimeter, PCFC and LOI for TPU and formulations (standard deviation given for selected parameters).

Materials	Mass loss calorimeter parameters				PCFC parameters		LOI (%) at 20°C
	Time to ignition (s)	pHRR (kW/m <sup>2</sup> )	THR (MJ/m <sup>2</sup> )	pHRR reduction (%)	pHRR (W/g)	THR (kJ/g)	
TPU	60±8.2	426±12.0	83.8±1.1	-	356±5.4, 417±7.5	25.7±1.1	23
L1-TPU	65±9.1	310±13.2	55.1±1.2	27	406±9.4	24.9±1.4	23
L2-TPU	115±8.3	266±14.2	53.2±1.4	37	355±6.1, 413±7.2	23.1±1.2	24
L3-TPU	60±8.0	279±13.1	54.6±1.2	34	357±6.0, 412±8.2	22.7±1.3	28

In order to understand this interaction, experimental and theoretical TGA curves were computed.<sup>25a</sup> Figure S1 shows the TGA curves of additives<sup>24</sup>, formulations, neat TPU and theoretical curves of the mixture. The difference between the experimental and theoretical TGA curves on formulations gives information on the reactivity of additives with TPU. If the experimental curve is above the theoretical one, the loss of weight is lower than expected, showing synergistic interaction of additives with polymer that leads to a thermal stabilization of the formulation. If the experimental curve is below the theoretical one, the reactivity of the polymer with additive leads to a thermal destabilization of the formulations.<sup>25a</sup> It can be seen from Figure S1 that L2 and L3 in TPU stabilize the degrading matrix at higher temperature (above 290°C). Considering high thermal instability of L1, there is gain in thermal stability in L1-TPU as judged from theoretical curve but fails at later stage due lack of char formation. The weight loss difference between the theoretical and the experimental TGA curve is also presented in Figure S1. In case of L2-TPU, the difference between the calculated and experimental weight loss becomes larger (> 30%) over a wider temperature range (330-400°C), an indication of char forming stage. L3-TPU although has ability to form char its efficiency is lower than L2-TPU.

Neat TPU in DSC (Figure 4b) shows a broad endothermic signal around 177°C due to disordering of HS crystallites.<sup>25b</sup> The signal at 213°C corresponds to melting of hard segment of TPU. In the cooling mode an exothermic peak is observed (~81

°C) due to crystallization. This profile is nearly followed in formulations (Table 1) with slight change in peak position. The shift in crystallization temperature is prominent in L2 and L3 based formulations due their supramolecular associations of hydroxyl groups with the matrix. The broad peak observed during heating around 85°C is due to softening temperature of TPU.

### 3.4. Material's response to simulated fire scenario

Flammability characteristic of TPU and flame retarded formulations are evaluated from rate of heat release (HRR) curves derived from two different techniques - Pyrolysis combustion flow calorimetry (PCFC) and Mass loss calorimetry (MCC) and are displayed in (Figure 5ab) with their associated parameters in Table 2. Neat TPU under cone calorimetry condition (35kW/m<sup>2</sup>) burns easily and to the full extent resulting in small amount of char (pHRR, 426 kW/m<sup>2</sup>). On the other hand in formulations (L2-TPU and L3-TPU), bubbling is seen at the beginning which soon collapse to form protective char layer and swells by the blowing action of gases released underneath. These events influence ignition time and pHRR value. Order of efficiency is in the order L2-TPU ≈ L3-TPU > L1-TPU > TPU in terms of reduction in pHRR. Although both L2-TPU (pHRR, 266 kW/m<sup>2</sup>) and L3-TPU (pHRR, 279 kW/m<sup>2</sup>) perform well in terms of reduction of total heat release but it is L2-TPU which in addition significantly extend the ignition time (115s).

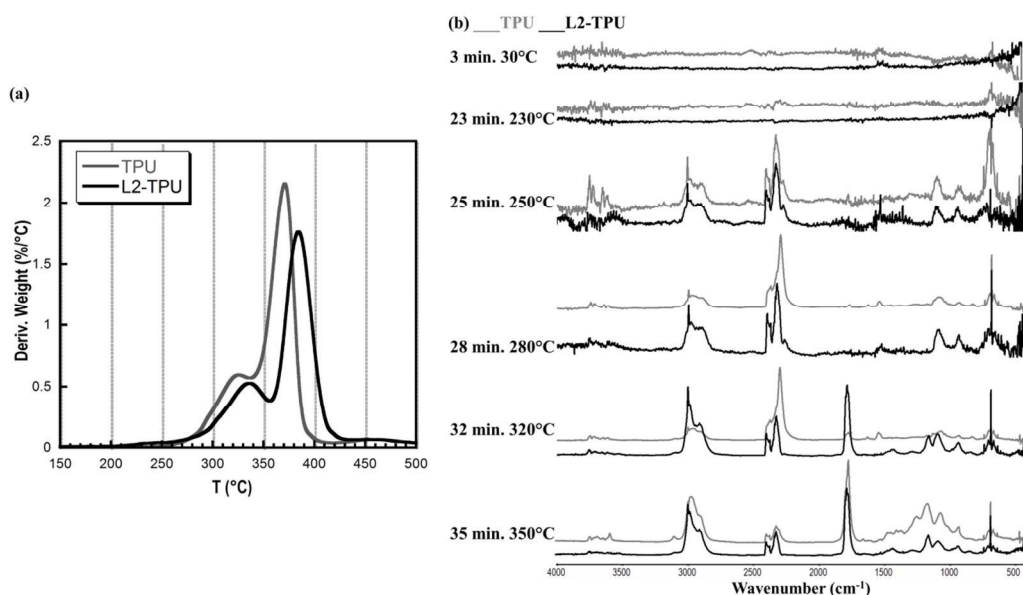


**Figure 6.** (a) TGA weight loss derivative curve. (b) Selected FTIR of L2-TPU and neat TPU recorded during simultaneous TGA run.

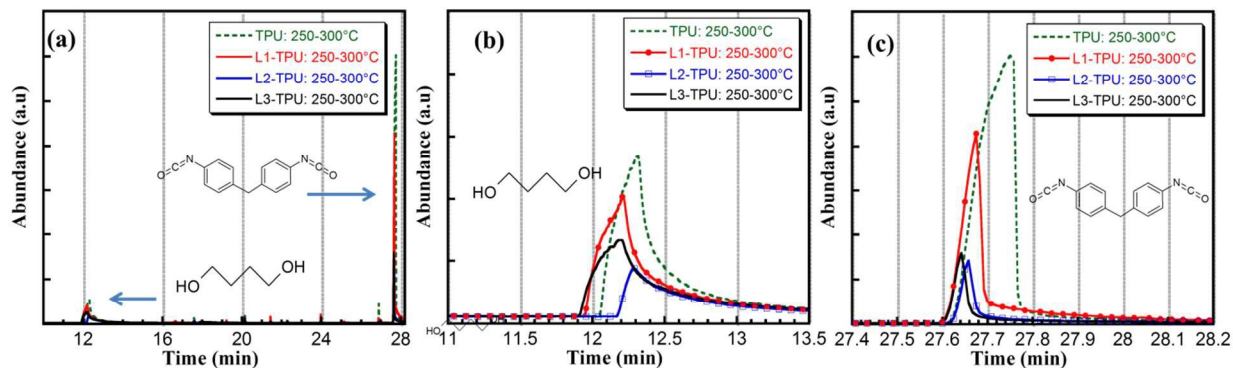
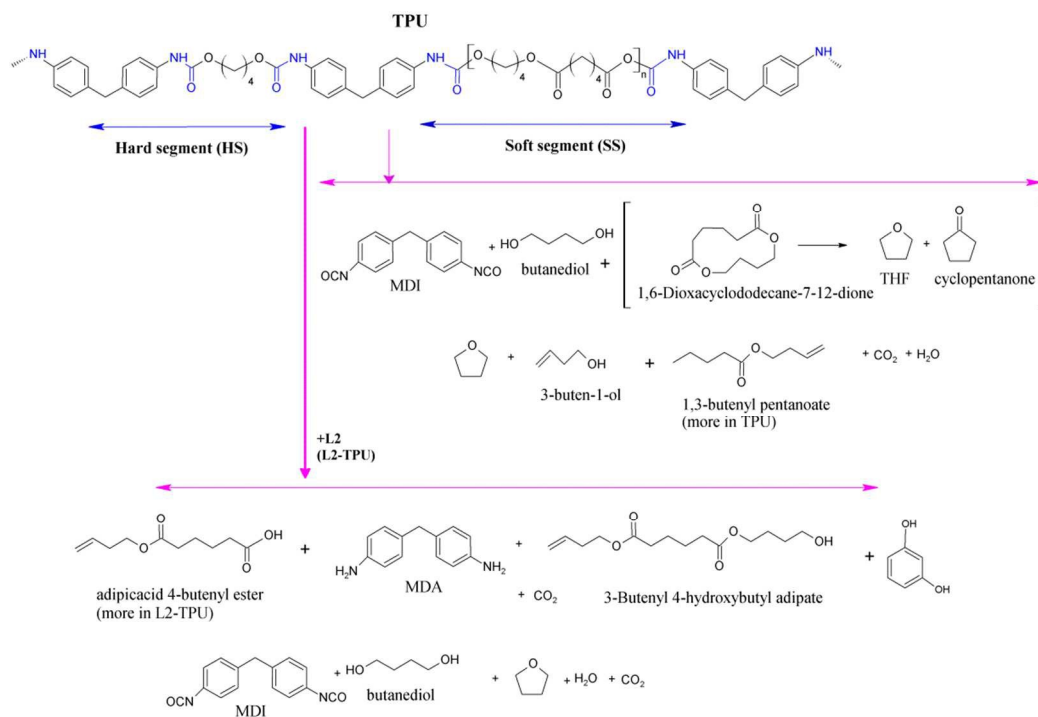


**Figure 7.** pyGCMS desorption experiment between 250-350°C focusing on evolution of butanediol and MDI.

HRR curve (Figure 5b) from PCFC for TPU shows two stages of heat release peaks (at 356 and 417°C) the profile of which nearly matches to that of thermal degradation curve (from TGA) having two unequal degradation steps. Formulations based on L2 and L3 follow the same trend but with reduction in pHRR in the first step (up to 33%) whereas it is marginal (13%) in the second step. FTIR on residue collected at 360°C (end of

1st degradation) confirms that it is indeed the HS that has been eliminated at this stage as  $\nu(\text{C}=\text{O})$  and  $\nu(\text{NH})$  of urethane group disappears. Unlike L2-TPU and L3-TPU, L1-TPU deviates (see PCFC) from the trend and undergoes single stage decomposition likely to be due to high sublimation probability of L1.



**Scheme 1.** Thermal degradation products in TPU and L2-TPU as evaluated from pyGCMS and supported TGA-FTIR in gas phase. For complete list of products refer Table S1.

PCFC recorded (Figure S2) on neat L2 and L3 shows pHRR in the temperature range that corresponds to their respective decomposition steps in TGA (Figure S1). The band in L2 (pHRR, 34 W/g) and L3 (112 W/g) means their individual contribution to pHRR but it is not so evident in their formulation counterparts except a small hump at the onset of HRR curve around 260°C.

There are also differences in limiting oxygen index (LOI) results among these formulations (Figure 5c-f). No improvement of LOI value is found in L1-TPU (LOI, 23%) which shows only dripping. The increase of LOI in L2-TPU is marginal (24 %) wherein it performs by char formation (Figure 5e) whereas the increase although significant (28%) in L3-TPU works mainly by dripping (Figure 5f). Thus based on physical response in LOI and variation in HRR curve it is presumed that L1-L3 follow different mode of action. The convenient protocol to investigate the flame retardancy mechanism is to follow the chemical species generated/transformed/released in condensed and/or gas phases during the simulated fire scenario like in cone calorimetry. As HRR curve witness the decomposition pathway, analysis of samples at different stages of this curve (like beginning, peak, end of decomposition) gives valuable information to understand decomposition mechanism of the polymer/formulation. Operando techniques like TGA-FTIR and py-GCMS wherein volatile species are detected and analyzed should provide information on gas phase action.

### 3.5. Gas phase analysis

#### 3.5.1. TGA coupled FTIR

**Neat TPU:** As discussed in the previous section TPU decomposes mainly in two overlapping steps. The volatile species evolved in these regions are detected by continuously monitoring by TGA coupled FTIR. Some selected FTIR are shown in figure 6. Until 23 min (230°C) no significant species are detected. Thereafter slowly CO<sub>2</sub> (2371, 2308, 670 cm<sup>-1</sup>) begin to evolve. Along with it hydrocarbons (2998-2874 cm<sup>-1</sup>), possibly species containing terminal -C-OH or C-O-C group (1079 and 912 cm<sup>-1</sup>) and hydroxyl species (bands above 3594 cm<sup>-1</sup>) are detected. Based on the reported<sup>20,21</sup> data it can be assumed that these bands are mainly due to butanediol evolved in this region. Between 280°C (28 min) to 320°C (32 min) there is considerable increase of a band at 2279 cm<sup>-1</sup> which is characteristic of -NCO group along with bands for butanediol. This corresponds to the beginning of the first major decomposition step and this is due to urethane dissociated product methanediphenyl diisocyanate (MDI).<sup>2,14</sup> As the thermal degradation enters second major degradation step (35min and until 41 min, 412 °C), isocyanate begins to decrease at the expense of strong hydrocarbon and carbonyl (1760 cm<sup>-1</sup>) bands (possibly cyclopentanone, a cyclized product or linear esters fragments from soft segment of TPU) which considerably increases.

## ARTICLE

**L2-TPU:** The onset of degradation here begins slightly early but the detected species are essentially similar to TPU degradation product (until 31 min, 310°C). This tentatively reveals that mode of onset of polymer dissociation is similar in both cases. In the following step, (31-36 min, 310-360 °C), signals for hydrocarbon and carbonyl group increases at the expense of CO<sub>2</sub> much similar to neat TPU but differ with respect to their time of evolution. This could be due to -NCO species involving in crosslinking/dimerization process of char formation or there may be multiple modes of polymer dissociation which are discussed in later section<sup>2,8</sup>. It has to be noted that TPU can dissociate in several ways.<sup>2,14</sup>

### 3.5.2. Pyrolysis GCMS:

**Desorption studies:** The temperature regions selected for this study is based on TGA pattern: 150-250°C; 250-300°C; 300-350°C; and 350-450°C. The first two temperature region corresponds to gradual minor weight loss steps that should reveal the mode of dissociation of TPU matrix. Analysis between 350-450°C corresponds to major degradation steps and mainly concerned with both primary and secondary degradation products of dissociating fragments of HS/SS. Identified products are summarized in table S1. For neat TPU until 250°C, trace amount of water, CO<sub>2</sub>, butanediol, methanediphenyl diisocyanate (MDI), tetrahydrofuran (THF), and a cyclic product 1,6-dioxacyclododecane-7-12-dione are identified.<sup>14</sup> On the other hand, along with these species, 4,4'-diaminodiphenylmethane, 3-Butenyl 4-hydroxybutyl adipate are detected in L2-TPU in the first step. Amine and olefin products are known to result from another degradation pathway of urethane group of TPU meaning operation of more than one type dissociation mechanisms in L2-TPU.

In the next step (250-300°C), the dominant species in TPU are 1,4-butanediol and MDI. These products are signature of urethane dissociation mechanism involving release of isocyanate and alcohol. It is found that amount of these two main degradation products are significantly reduced in the formulations (Figure 7b,c). This observation was also made in TGA-FTIR. THF and cyclopentanone are also detected in both cases at this stage which are formed from dehydration-cyclization of (1,4-butanediol and adipic acid components) 1,6-dioxacyclododecane.<sup>14</sup> It is also found that products identified in the next two steps are similar among TPU and formulations and are much complicated due to numerous break-down,

cyclized products in all formulations. Fragments of additives like resorcinol, benzoquinone and salicylaldehyde are also identified (in <250°C range) in case of L2-TPU, L3-TPU and L1-TPU respectively. Although ethylenediamine and its deamination product pyrazine are identified during the desorption experiment in neat L2 they are not traced in formulation.<sup>24</sup>

**Pyrolysis studies (at 600°C):** Pyrolysis at 600°C which corresponds to completion of degradation in formulations provides additional information. Although it is not the scenario of cone calorimetry, the material is subjected directly to high temperature like in some fire scenario (e.g. open flame impinging the material). Some of the products identified (H<sub>2</sub>O, CO<sub>2</sub>, THF, cyclopentanone) at 600°C are similar in TPU and L2-TPU whereas more of MDI, hydrocarbons, short chain ester fragment of 1,3-butenyl pentanoate (m/z, 156) and cyclized molecule like 1,6-dioxacyclododecane are found in TPU. Larger ester fragments like adipic acid 4-butenylester (m/z, 200) and 3-dibutenyl adipate (m/z, 254) are found to be dominant in L2-TPU. Scheme 1 depicts an overview of tentative degradation products in TPU and L2-TPU. Product formation and detection is influenced by heating rate, column temperature, polarity of eluting molecules, interference with other products, adsorption on column, gas-phase interaction, and secondary degradations. Despite this a good correlation is found from TGA-FTIR and pyGCMS results.

### 3.6. Condensed phase analysis by <sup>13</sup>C MAS NMR and FTIR studies.

We have seen in mass loss calorimetry experiment that formulations swells and consequently forms char under heat flux. TPU itself being least contributor to intumescence/char, the observed intumescence/char is expected to be from additives or influence of additives on HS/SS of TPU. The exact way of its contribution could be evaluated from condensed phase analysis. As explained in experimental section, samples for condensed phase analysis were collected based on HRR curve which represents different stages of degradation. Analysis of samples at the onset, peak, descending and end of decomposition normally should provide useful inputs to reveal the degradation mechanism. FTIR and <sup>13</sup>C MAS NMR are routine technique to probe these degradation steps.

## ARTICLE

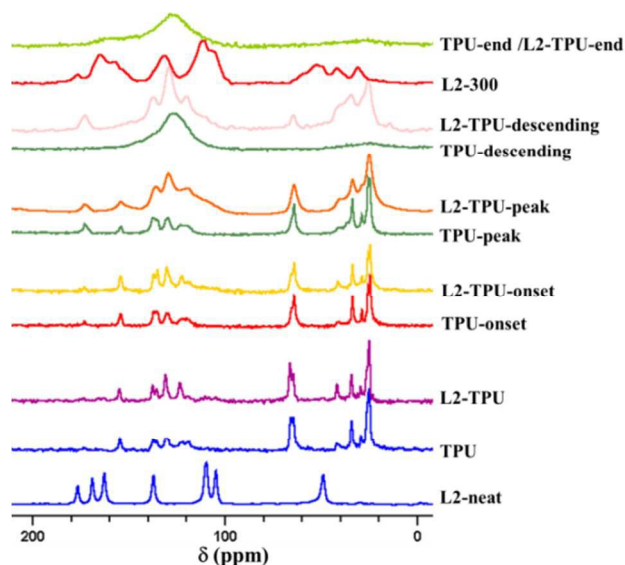


**Figure 8.**  $^{13}\text{C}$  MAS NMR on TPU and L2-TPU at different degradation steps (onset, peak, descending and end refers to samples collected from mass loss calorimetry based on HRR curve which are at different stages of decomposition; L2-300 is a stage<sup>24</sup> in the thermal decomposition of L2).

Since additive signals due to its smaller dosage are not distinctly seen in MAS  $^{13}\text{C}$  NMR or FTIR and some of the signals are overlapped by dominant TPU signals tracking the

degradation mechanism difficult. Despite this following noticeable changes are seen particularly in samples collected at peak of degradation and at later stages. As an example a comparative figure is given (Figure 8) showing TPU and L2-TPU at different stages of degradation. In L2-TPU-peak, the region between 115-140 ppm characteristic of aromatic carbons in neat TPU becomes considerably broader (stretches between 100-150 ppm) with variation in intensity. Indeed aliphatic region also has seen some changes. There is an additional band around 40ppm appeared as a shoulder on the degrading aliphatic fragments from TPU (Figure 8). Both these changes (in aromatic and aliphatic regions) are thought to be brought about by additives. Since both the regions are overlapped by still remaining degrading TPU components no conclusive evidence on fate of additive is drawn-out. Since decomposition of neat TPU also stretches over a period of temperature the crucial information in the initial stages of additive structure-functioning escape detection. Sample collected at the descending part of the HRR curve also provides limited information being similar to L2-TPU-peak. Formation of char is confirmed in the residue with a broad signal around 125 ppm. The peak at 175 ppm might be due to some carbonyl species that may have origin from oxidation of methylene chain or some cyclized carbonyl species.

Selected FTIR spectra of L2-TPU degradation are given in figure 9. Only expanded region is shown as region above  $2700\text{ cm}^{-1}$  is not quite well resolved. Spectrum of L2-TPU is not shown as it closely resembles L2-TPU-onset.

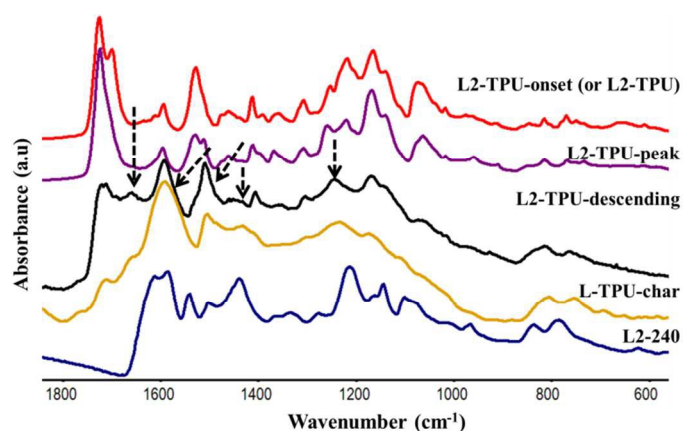


**Figure 9.** Expanded part of FTIR on samples (L2-TPU) collected from mass loss calorimetry (onset, peak, and descending refers to samples collected based on HRR curve which are at different stages of degradation). Arrow indicates new bands in L2-TPU-descending). L2-resin formation around  $240^\circ\text{C}$  (L2-240) is also shown for comparison.<sup>24</sup>

## ARTICLE

It can be seen that in L2-TPU-peak it is carbonyl stretching ( $1704\text{ cm}^{-1}$ ) of urethane group that undergoes reduction in intensity confirming our earlier observation that HS is the preferred choice of cleavage.<sup>11,12,16</sup> FTIR spectrum of L2-TPU-descending shows several new bands at  $1661\text{m}$ ,  $1592\text{s}$ ,  $1509\text{s}$ , multiplets around  $1452\text{m}$ ,  $1246\text{m}$ , and  $813\text{br cm}^{-1}$ . The first four signals are assigned to the formation of new aromatic structure possibly involving additive framework. This was concluded because as the other aromatic contributor MDP (from TPU) decompose completely by this stage. The signal at  $1452\text{cm}^{-1}$  together with signal at  $40\text{ppm}$  in  $^{13}\text{C}$  MAS NMR indicates formation of new aliphatic fragments.

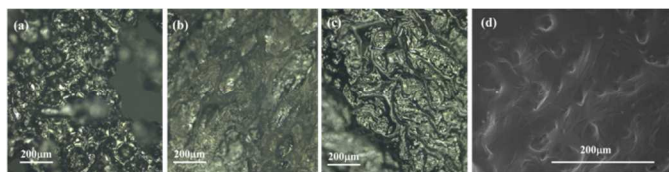


**Figure 10.** Optical microscope images on residues (surface) collected in cone calorimetry experiments (a) TPU (b) L2-TPU (c) L3-TPU (d) SEM image on residue of L2-TPU showing scattered aggregates of resins.

It is also possible that both new aromatic and aliphatic signals are arising from the same framework and likely from chemical modification of additive as most of the TPU framework is destroyed at this stage. This is evident from decrease or disappearance of several bands in FTIR spectrum. The molecules at this stage are possibly one among several species down the chain of reactive chemicals, a contributor to cross-linker and char former. In order to retrieve these masked species and their precursors it is necessary to compare with the thermal behavior of L2 which was investigated by us.<sup>24</sup> It was found that L2 upon thermal treatment undergoes polycondensation via covalent cross-linking forming hyperbranched cross-linked resins much similar to phenolic resins.<sup>27-34</sup> The active molecule involved in this process is assumed to be resorcinol from the breakdown product of L2. Methylene bridge formation is conclusively confirmed by FTIR and solid state NMR which is in close alignment with that observed in the present case. These resorcinol based resins favor the formation of intumescence and char.

It was also found that the poly-condensation sites differ in L2 and L3 which involve novolac and resol type resin formation respectively.<sup>24</sup> Formation of phenolic resin are also observed in L3-TPU as evidenced by FTIR and MAS NMR (Figure S3 and S4). In this respect it is worth mentioning a recent study of self-

polymerisation of resole type prepolymer in blocked polyurethane which forms interpenetrating polymer network of blocked polyurethane and phenolic resin.<sup>36</sup>

L1, the unsubstituted Saline molecule used in the present study although still hold promise because of its limited performance has high inclination for sublimation and lower thermal stability could not hold up to the expectation. Moreover, salicylaldehyde, a breakdown product of L1 is not a solid unlike resorcinol or hydroquinone and vaporizes easily.

### 2.7. Texture studies

Optical microscopic images on residue (on surface) were displayed in figure 10. Residue from TPU shows a hexagonal cellular structure which are loosely held. Char surface of L2-TPU shows slightly elongate cellular structure with thick walls occasionally ruptured creating pores. But this char formation is peculiar in the sense it is multilayered, strong, but less-flexible. L3-TPU shows more elongated cellular structure with slightly shiny surface. Each cell bear numerous folding, flexible, single layered and moderately strong. It can be recalled that L2 residue possess nitrogen in variable amount.<sup>24</sup> This is partially attributed to in situ formation of benzoxazine type resins. Considering the advantages of polybenzoxazines over traditional phenolic resins these observations are significant as also noted in reported poly(urethane-benzoxazine) films as novel polyurethane/phenolic resin composites.<sup>35</sup> However EPMA (not shown) on L2-TPU-800 did not show any evidence of presence of nitrogen thus concluding that char is mainly composed of phenolic resin and no traces of benzoxazine type resin.

### 3.8. Mapping the degradation mechanism of additive blended TPU

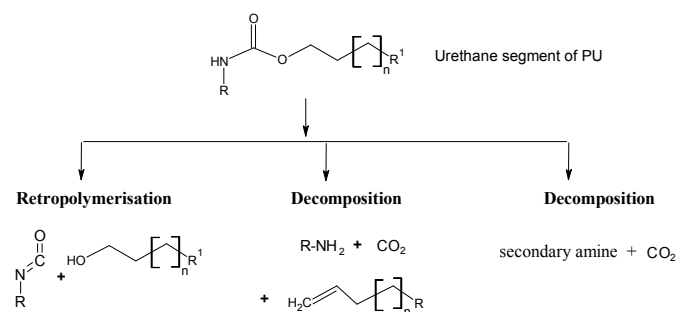
In thermal decomposition (thermolysis) of TPU, the weakest point of the polyurethane chain is the urethane group.<sup>15</sup> Thermal decomposition of TPU proceeds mainly through 2 steps. The first step is the degradation of hard segment followed by the decomposition of soft segment. There are three main pathways for the initial degradation of the urethane linkage (Scheme 2). Depolymerization into isocyanate and alcohol; dissociation into primary amine, olefin, and  $\text{CO}_2$ ; formation of secondary amine with elimination of  $\text{CO}_2$ . Additives often influence these paths and polymer may adopt any of these routes or more likely combination of them. From FTIR we found that Schiff base (L2 and L3) establish H-bonding interactions with urethane segment (Figure 3a) in L2-TPU and L3-TPU and thus assumed to have influence on TPU dissociation process.

## ARTICLE

Although there is early onset of TPU break down (see TGA) in formulations the subsequent process is gradual stretching the complete degradation of TPU. We have seen in the previous section and in our earlier work<sup>24</sup> how resorcinol or hydroquinone component of L2 or L3 respectively can contribute to char formation. Resorcinol or 2,4-dihydroxybenzaldehyde alone due its high sublimating tendency at higher temperature fails to build-up resin/char. Stabilizing such hydroxyphenols by structuring into Schiff bases is an alternative approach which can influence their sublimation rate, control release, resin formation, and thermal stability. Recent work shows that in the derived form like in resorcinol bis(diphenyl phosphate), it was found to be an efficient flame retardant.<sup>37</sup> Resorcinol or benzoquinone are known to be radical scavengers that could be released from L2 and L3 respectively and may act both in gas phase and condensed phase.<sup>22,23,38</sup> The additive L2 is found to release (from pyGCMS) small amount of resorcinol in the gas phase during the curing process which may fractionally contribute to the radical quenching chemistry of gas phase action of flame retardancy. As TPU itself is thought to contribute to the oxidation by producing either OH radicals<sup>2</sup> or water which may act as oxidizing agent, any free resorcinol trapped in condensed may also act as radical scavenger. On the other hand its sublimation causes blowing action which partly made char surface to swell increasing the gap between burning and unburnt polymer. Additives promote both segments of TPU to contribute to char formation either actively or passively. From TGA-FTIR, pyGCMS and analysis of residue from PCFC by FTIR (~360°C) indicate that HS of neat TPU decomposes first followed by SS. MDI and butanediol results from HS while a cyclized species mainly 1,6-dioxacyclododecane results from SS. Neat TPU has high inclination for formation of cyclized product from SS segment which degrades to smaller fragments like cyclopentanone, butanediol, pentanoic acid and 1,3-butenyl pentanoate. L2-TPU does not seem to favor cyclic products but utilizes SS. It is reported that ester segment of the TPU chain can bind to phenolic resin<sup>22</sup> during its resin formation for cross-linking. Thus L2-TPU at higher temperature is found to release larger fragments like, adipic acid, 4-butenylester and 3-dibutenyladipate (Scheme 1) which are considerably less in neat TPU. These species pass through stages like formation of diene, polyene, polyaromatics before forming char (Scheme 3).<sup>2</sup>

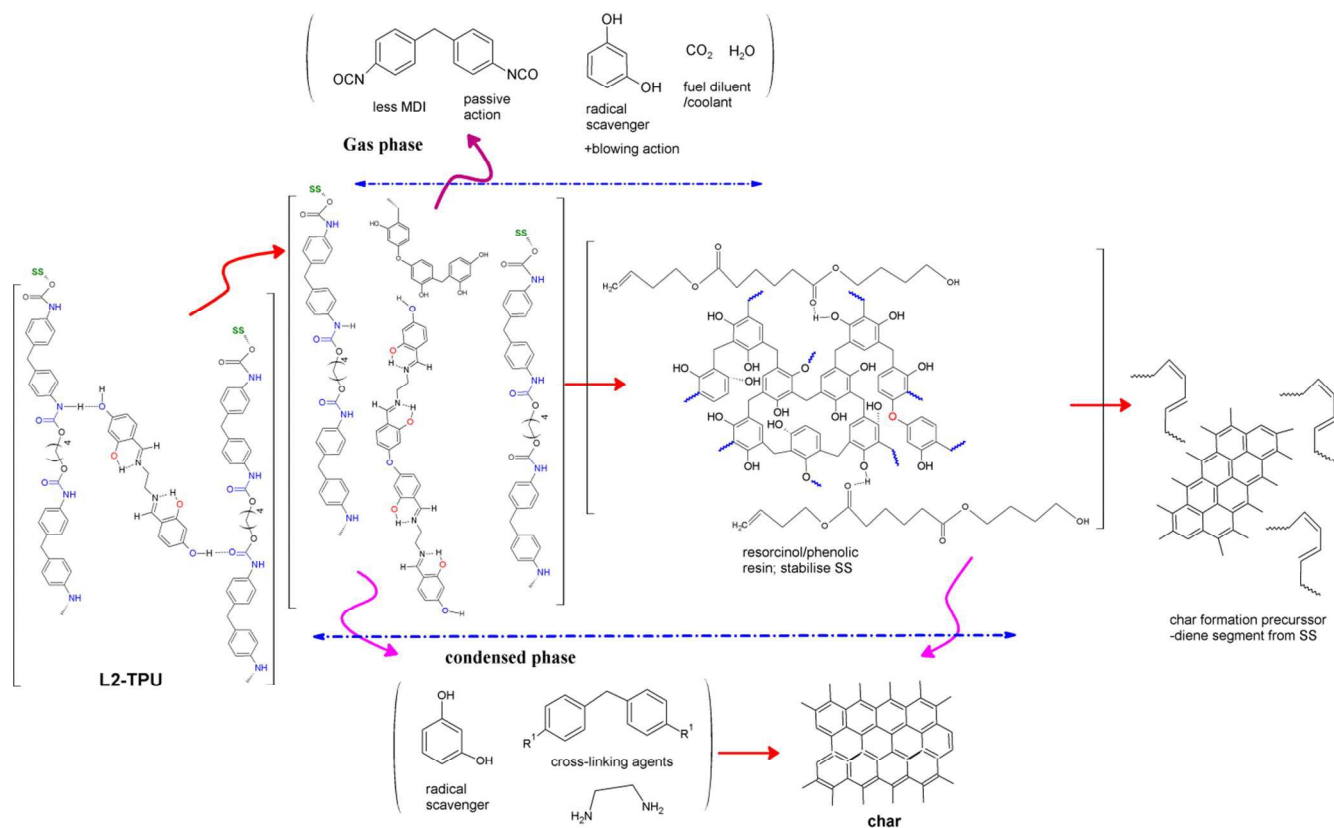
Isocyanate production in TPU degradation is not considered favorable due to environmental issues.<sup>20</sup> On the other hand its high reactivity and cross-linking ability are positive aspects to exploit it towards char formation in the condensed phase if

suitable reactants are made available. From TGA-FTIR and pyGCMS it was tentatively estimated that diisocyanate (MDI) evolution in the gas phase is considerably lowered in formulations possibly reducing the pHRR of PCFC curve. Several reasons are reported for such decrease in the evolution of isocyanate and discussed in the following section.<sup>2,16,20</sup>



**Scheme 2.** Possible thermal degradation routes of urethane segment of polyurethane.

The interference of additive in the urethane dissociation stage (Scheme 2) may modify the usual retropolymerisation process decreasing MDI production. The -OH groups of free resorcinol from disjointing L2 or L3 may reacts with released highly reactive diisocyanates. This leads to isocyanate-derived cross-links which are more robust and more resistive to shrinkage like in case of carbon aerogels.<sup>22</sup> Phenolic hydroxyls can also react with isocyanates to form carbamates. The isocyanates formed may be dimerised to carbodiimide or undergo trimerization leading to isocyanurate are also reported.<sup>2</sup> These species may react with remaining urethane groups or polar groups on polyester chain to form a cross-linked structure. We have seen that during cross-linking or curing of resorcinol from Schiff base, a highly branched interconnected resorcinol/phenolic resin is formed by polycondensation reaction between the phenolic prepolymer units.<sup>24</sup> This cross-linking/resin formation density found in neat L2 not necessarily be the same in TPU matrix as TPU matrix may reduce cross-link density of this resin allowing additional reaction between resin and ester fragment of hard segment similar to that taking place in resorcinol-formaldehyde (RF) resins in polyester.<sup>22</sup> Nevertheless the major flame retardancy action in this Schiff base flame retarded TPU is in the condensed phase by intumescence via resin intermediate which acts as physical defensive barrier.



**Scheme 3.** A simplified tentative degradation mechanism showing active and passive species responsible for flame retardancy in L2 blended TPU ( $R^1 = -NCO$  or  $-NH_2$  group; SS=soft segment).

This tightly cured bonding network of aromatic phenolic resin slows down heat and mass transfer between gaseous and condensed phases and thus retards the degradation and acts as heat shield. A key characteristic of such thermoset phenolic resin is its ability to withstand high temperature. Cured phenolic resin also provides the rigidity necessary to maintain structural integrity and dimensional stability of char which in its absence leads to feeble char. Thus Salen Schiff base that mimic the thermosetting behavior of resorcinol/phenol resin plays a pivotal role in this flame retardancy of action.

#### 4. Conclusions

Schiff bases are the most versatile molecules among organic compounds finding diverse application like catalysis, medicine, molecular sensors, as ligands in coordination chemistry, magnetic materials to name some but rarely leaped into high temperature applications. This was partially due to the perception about 'Salen' molecules as a 'soft' molecular framework. Our investigation reveals for the first time that such molecules can be used for high temperature applications. This can be further improved by modifying the framework of the 'Salen' molecules and can be structure tuned to improve the

performances. For example, L2/L3 which bear hydroxyl substitution is found to perform better than their unsubstituted counterpart, L1 and thus seemingly outperform L1-TPU. The observed flame retardancy of L2-TPU is mainly credited to the char forming ability of L2 as it endorses phenolic resin formation thus upcoming of new generation intumescence promoting FRs. The remote possibility of radical chemistry of flame quenching by L2 or L3 in the gas phase also cannot be excluded. It is worth to mention that intumescence observed in the present case works without any acid source or any synergist. The scope for this type of additives is enormous as there is large scope for redesigning this molecule and further stabilizing by known flame retardant active cations (Al, Zn..) or anions (phosphate, borate) by encapsulation.

#### Acknowledgements

Authors would like to thank Mr. Bertrand Doumert for his assistance during MAS NMR recording.

#### Notes and references

<sup>a</sup>ISP/UMET – UMR/CNRS 8207,  
Ecole Nationale Supérieure de Chimie de Lille (ENSCL),  
Avenue Dimitri Mendeleïev – Bât. C7a, BP 90108, 59652  
Villeneuve d'Ascq Cedex, France  
E-mail: [serge.bourbigot@ensc-lille.fr](mailto:serge.bourbigot@ensc-lille.fr)

Electronic Supplementary Information (ESI) available that includes identification of pyrolysates (Table S1); Experimental and theoretical TGA curves (Figure S1); PCFC (Figure S2); TGA-FTIR (Figure S3); <sup>13</sup>C MAS NMR on L3 (Figure S4); FTIR on L3 (Figure S5).

#### References:

- S. Duquesne, Michel Le Bras, Serge Bourbigot, René Delobel, Giovanni Camino, Berend Eling, Chris Lindsay, Toon Roels and Hervé Vezin, *J. Appl. Poly. Sci.*, 2001, **82**, 3262.
- D.K. Chattopadhyay, Dean C. Webster, *Prog. Poly. Sci.*, 2009, **34**, 1068.
- D. Tabuani, F. Bellucci, A. Terenzi, G. Gamino, *Polym Degrad. Stab.*, 2012, **97**, 2594.
- G. Fontaine, T. Turf, S. Bourbigot, *Fire and Polymers V*, Chapter 20, ACS symposium, 2009, 1013, 329.
- <http://www2.basf.us/urethanechemicals/tpu/pdf/C85A.pdf>
- S. Bourbigot, M. Le Bras, and J. Troitzsch, *Fundamentals: introduction*, in: J. Troitzsch, (Eds), *Flammability handbook*, Munich, Hanser Verlag, 2003, 3-7.
- C.A. Wilkie, and A.B. Morgan, *Fire Retardancy of Polymeric Materials*, Second Edition, CRC Press, ISBN: 978-1-4200-8399-6, 2009.
- B. Scharrel, *Materials*, 3 (2010) 4710.
- T.R. Hull, and B. Kandola, (Eds), *Fire retardancy of polymers: New strategies and mechanisms*. RSC Publishing, ISBN: 978-0-85404-149-7, 2008.
- Dan Rosu, Nita Tudorachi, Liliana Rosu, *J. Anal. Appl. Pyro.*, 2010, **89**, 152.
- J.M. Cervantes-Uc, J.I. Moo Espinosa, J.V. Cauich-Rodríguez, A. Ávila-Ortega, H. Vázquez-Torres, A. Marcos-Fernández, J. San Román, *Poly. Deg. Stab.*, 2009, **94**, 10, 1666.
- M. Herrera, G. Matuschek, A. Kettrup, *Poly Deg Stab*, 2002, **78**, 323.
- A. Konig, U. Fehrenbacher, T. Hirth and E. Kroke, *J. Cellular plastics*, 2008, **44**, 464.
- Byoung-Hyoun Kim, K.Yoon, D. Cheul Moon, *J. Anal. Appl. Pyro.*, 2012, **98**, 236.
- J. Simon, F. Baria, Anna Kelemen-Haller, F. Farkas, Marta Kraxner, *Chromatographia*, 25, 1988, 99-106.
- M. Berta, C. Lindsay, G. Pans, G. Camino, *Poly. Deg. Stab.*, 2006, **91**, 1179.
- W.P. Yang, C.W. Macosko, S.T. Wellinghoff, *Polymer*, 1986, **27**, 1235.
- A. Toldy, Gy. Harakaly, B. Szolnoki, E. Zimonyi, Gy. Marosi, *Poly. Deg. Stab.*, 2012, **97**, 2524.
- G. Trovati, E. Ap Sanches, S. Claro Neto, Y.P. Mascarenhas and G.O. Chierice, *J. Appl. Poly. Sci.*, 2010, **115**, 263.
- X. Chen, L. Huo, C. Jiao, S. Li, *J. Anal. and applied Pyrolysis*, 2013, **100**, 186.
- P.-S. Wang, *Poly. Deg. Stab.*, 1999, **66**, 307.
- Resorcinol: Chemistry, Technology and Applications*, Raj B. Durairaj, Springer, 2005, ISBN: 3540251421.
- V. Thavasi, R. Phillip A. Bettens, Lai Peng Leong, *Phys. Chem. A*, 2009, 113 (13), 3068.
- A. D. Naik, G. Fontaine, S. Bellayer, S. Bourbigot (in preparation)
- (a) M. Jimenez, S. Duquesne, S. Bourbigot, *Thermochim. Acta*, 2006, **449**, 16. (b) A. Frick, A. Rochman, *Polymer testing*, 2004, **23**, 413.
- Y. Zhu, J. Hu, Ka-Fai Choi, Kwok-Wing Yeung, Q. Meng, S. Chen, *J. Appl. Poly. Sci.*, 2008, **107**, 599.
- L. Costa, L. Rossi di Montelera, G. Camino, E.D. Weil, E.M. Pearce, *Poly Deg. Stab.*, 1997, **56**, 23.
- S. Mulik, C. Sotiriou-Leventis, N. Leventis, *Chem. Mater.*, 2008, 20 (22), 6985.
- L. B. Manfredi, D. Puglia, J. M. Kenny, A. Vazquez, *J. Appl. Poly. Sci.*, 2007, **104**, 3082.
- Marie-Florence Grenier-Loustalot, S. Larroque, P. Grenier, *Polymer*, 1996, **37**, 639.
- Sheng Lin-Gibson, PhD thesis, 2001, *Cresol novolac/epoxy networks: synthesis, properties and processability*. <http://vtechworks.lib.vt.edu/handle/10919/27296>.
- W. Hesse, J. Lang, *Phenolic resins, Ullmann's Encyclopedia of Industrial Chemistry*, 2000, **26**, 583.
- E. Fitzer and W. Schafer, *Carbon*, 1970, **8**, 353.
- S. Zeng, L. Guo, L. Zhang, F. Cui, J. Zhou, Z. Gao, Yu Chen and J. Shi, *Macromolecular Chemistry and Physics*, 2010, **211**, 845.
- T. Takeichi, Y. Guo, T. Agag, *J. Polym. Sci.*, 2000, **38**, 4165.
- Y.-Y. Sun, C.-H. Chen, *Polymer Eng. Sci.*, 2011, **51**, 285.
- K.H. Pawlowski, B. Scharrel, *Polymer International*, 2007, **56**, 11, 1404.
- D. Mikulski, R. Górnica, M. Molski, *Eur J. Med. Chem.* 2010, **45**, 1015.